Qiao, L., Wang, X., Smith, P., Fan, J., Lu, Y., Emmett, B., Li, R., Dorling, S., Chen, H., Liu, S., Benton, T. G., Wang, Y., Ma, Y., Jiang, R., Zhang, F., Piao, S., Müller, C., Yang, H., Hao, Y., Li, W., Fan, M. (2022): Soil quality both increases crop production and improves resilience to climate change. - Nature Climate Change, 12, 6, 574-580.

DOI: https://doi.org/10.1038/s41558-022-01376-8

Inventory of Supporting Information

NCLIM-21122311A: Soil quality both increases crop production and improves resilience to climate change.

Corresponding author name(s): Mingsheng Fan.

1. Extended Data

Figure #	Figure title One sentence only	Filename This should be the name the file is saved as when it is uploaded to our system. Please include the file extension. i.e.: *Smith_ED_Fig1.jpg*	Figure Legend If you are citing a reference for the first time in these legends, please include all new references in the main text Methods References section, and carry on the numbering from the main References section of the paper. If your paper does not have a Methods section, include all new references at the end of the main Reference list.
Extended Data Fig. 1	Yield under best management practices	Fan_ED_Fig 1.eps	a-c, wheat, d-f, maize, and g-i rice. The filled orange corresponds to a bar for each individual $Yield_{BMPs}$ site-year

	(Yield$_{BMPs}$)		(ranked from high to low, Numbers shown on each panel). The blue dashed lines indicate mean Yield$_{BMPs}$. Yield$_{BMPs}$ (Mg/ha) are shown as mean (±SD, standard deviation); Coefficient of variation (CV, %) calculated by dividing mean yield by SD; N refers to the number of site-years of on-farm trials in major cropping systems in China. W-NCP, winter wheat in North China Plain; W-YZB, winter wheat in Yangtze River Basin; W-NWC, winter wheat in Northwest China; M-NEC, rainfed maize in Northeast China; M-NCP, maize in North China Plain; M-SWC, rainfed maize in Southwest China; SR-YZB, single rice in Yangtze River Basin; ER-SC, early rice in South China; LR-SC, late rice in South China
Extended Data Fig. 2	The relative contribution (%) of explaining variables to yields under best management practices.	Fan_ED_Fig 2.eps	Assessment was conducted by Gradient Boosted Regression Tree models based on the primary data comprising all on-farm trials in major cropping systems in China. Orange, green and blue bars indicate climate, soil and management variables respectively. Tmax and Tmin, maximum and minimum temperature; PRE, precipitation; GDD, growing degree days; RAD, solar radiation; SOM, soil organic matter; Olsen-P and Avail-K, soil available phosphorus and potassium. W-NCP, winter wheat in North China Plain; W-YZB, winter wheat in Yangtze River Basin; W-NWC, winter wheat in Northwest China; M-NEC, rainfed maize in Northeast China; M-NCP, maize in North China Plain; M-SWC, rainfed maize in Southwest China; SR-YZB, single rice in Yangtze River Basin; ER-SC, early rice in South China; LR-SC, late rice in South China.

Extended Data Fig. 3	Geographical distribution of paired on-farm trials under high- and low-quality soils.	Fan_ED_Fig 3.eps	Symbols of blue dot and red triangle indicate on-farm trials conducted in high- and low-quality soils in major cropping systems in China, respectively. Paired on-farm trials were conducted in high-(N=1665) and low - (N=1676) quality soils. W-NCP, winter wheat in North China Plain; W-YZB, winter wheat in Yangtze River Basin; W-NWC, winter wheat in Northwest China; M-NEC, rainfed maize in Northeast China; M-NCP, maize in North China Plain; M-SWC, rainfed maize in Southwest China; SR-YZB, single rice in Yangtze River Basin; ER-SC, early rice in South China; LR-SC, late rice in South China.
Extended Data Fig. 4	Comparison of climate variables between locations of paired on-farm trials conducted in high- and low- quality soils.	Fan_ED_Fig 4.eps	a-d, average maximum temperature (a), average minimum temperature (b), cumulative precipitation (c) and cumulative radiation (d) between locations, where paired on-farm trials were conducted in high-(N=1665) and low - (N=1676) quality soils. W-NCP, winter wheat in North China Plain; W-YZB, winter wheat in Yangtze River Basin; W-NWC, winter wheat in Northwest China; M-NEC, rainfed maize in Northeast China; M-NCP, maize in North China Plain; M-SWC, rainfed maize in Southwest China; SR-YZB, single rice in Yangtze River Basin; ER-SC, early rice in South China; LR-SC, late rice in South China. *** refers to significance at $p = 0.001$.
Extended Data Fig. 5	Projected yield change in future climate change.	Fan_ED_Fig 5.eps	a,b, projected yield changes under RCP2.6 (a) and RCP8.5 (b) pathways up to 2040-2059; c,d, projected yield changes under RCP2.6 (c) and RCP8.5 (d) pathways up to 2080-2099. Projections were based on Gradient Boosted Regression Tree (GBRT) model trained on the primary data set comprising all

			on-farm trials for major cropping systems in China. Boxes represent variability across each cropping system over the 2040-2099 periods. Solid lines and diamonds in this figure indicate median and mean yields, respectively; the boundary of the box indicates the 25th and 75th percentile; whisker caps denote the 90th and 10th percentiles. W-NCP, winter wheat in North China Plain; W-YZB, winter wheat in Yangtze River Basin; W-NWC, winter wheat in Northwest China; M-NEC, rainfed maize in Northeast China; M-NCP, maize in North China Plain; M-SWC, rainfed maize in southwest China; SR-YZB, single rice in Yangtze River Basin; ER-SC, early rice in South China; LR-SC, later rice in South China.
Extended Data Fig. 6	Projected yield changes and their difference between high- and low-quality soils.	Fan_ED_Fig 6.eps	a-d, projected yield changes and their difference between high- and low-quality soils under climate change in RCP 2.6 (a) and RCP 8.5 (b) up to 2040-2059, and RCP 2.6 (c) and RCP 8.5 (d) up to 2080-2099. Projected yield changes were estimated based on the primary dataset comprising all on-farm trials, differences of yield changes were estimated based on sub-datasets comprising on-farm trials with paired high- and low-quality soils in major cropping systems in China. Horizontal and vertical error bars (standard deviation, SD) represent inter-annual variations of yield changes and difference of yield change between high- and low-quality soils, respectively. Solid lines represent significant difference in yield change between high- and low-quality soil at $p = 0.10$, while dashed lines represent no significant difference. W-NCP, winter wheat in

			North China Plain; W-YZB, winter wheat in Yangtze River Basin; W-NWC, winter wheat in Northwest China; M-NEC, rainfed maize in Northeast China; M-NCP, maize in North China Plain; M-SWC, rainfed maize in Southwest China; SR-YZB, single rice in Yangtze River Basin; ER-SC, early rice in South China; LR-SC, late rice in South China.

2. Supplementary Information:

A. Flat Files

Item	Present	Filename This should be the name the file is saved as when it is uploaded to our system, and should include the file extension. The extension must be .pdf	A brief, numerical description of file contents. i.e.: *Supplementary Figures 1-4, Supplementary Discussion, and Supplementary Tables 1-4.*
Supplementary Information	Yes	SI-NCLIM-21122311A. pdf	Supplementary Text S1 to S2, Supplementary Figures S1 to S7, and Supplementary Table S1 to S6.
Reporting Summary	Yes	Reporting summary-NCLIM-21122311A. pdf	

Soil quality both increases crop production and improves resilience to climate change

Lei Qiao[1,2], Xuhui Wang[3], Pete Smith[4], Jinlong Fan[5]， Yuelai Lu[6], Bridget Emmett[7], Rong Li[8], Stephen Dorling[9], Haiqing Chen[10], Shaogui Liu[11], Tim G. Benton[12], Yaojun Wang[13], Yuqing Ma[1,2], Rongfeng Jiang[1,2], Fusuo Zhang[1,2], Shilong Piao[3], Christoph Möller[14], Huaqing Yang[1,2], Yanan Hao[1,2], Wangmei Li[1,2], Mingsheng Fan[1,2*]

[1]College of Resources and Environmental Sciences, China Agricultural University, Beijing 100193, China; [2]National Academy of Agriculture Green Development, China Agricultural University, Beijing 100193, China; [3]Sino-French Institute for Earth System Science, College of Urban and Environmental Science, Peking University, Beijing 100871, China; [4]Institute of Biological and Environmental Sciences, University of Aberdeen, Aberdeen AB24 3UU, United Kingdom; [5]National Satellite Meteorological Center, China Meteorological Administration, Beijing 100081 China; [6]School of International Development, University of East Anglia, Norwich NR4 7TJ, United Kingdom; [7]UK Centre for Ecology and Hydrology, Environment Centre Wales, Bangor, Gwynedd, LL57 2UW, United Kingdom; [8]Cultivated Land Quality Monitoring and Protection Center, Ministry of Agriculture and Rural Affairs of the People's Republic of China, Beijing 100125, China; [9]School of Environmental Sciences, University of East Anglia, Norwich NR4 7TJ, United Kingdom； [10]College of Land Science and Technology, China Agricultural University, Beijing 100193, China; [11]Yangzhou Station of Farmland Quality Protection, Yangzhou 225101 China; [12]Royal Institute of International Affairs, Chatham House, London SW1Y 4LE, United Kingdom; [13]College of Information and Electrical Engineering, China Agricultural University, Beijing 100193, China; [14] Potsdam Institute for Climate Impacts Research, Member of the Leibniz Association, 14473 Potsdam, Germany.

[*] Correspondence author (fanms@cau.edu.cn).

Interactions between soil quality and climate change may influence the capacity of croplands to produce sufficient food. Here, we address this issue by using a new dataset of soil, climate and associated yield observations for 12115 **site-years representing 90% of total cereal production in China. Across crops and environmental conditions, we show that high-quality soils reduced the sensitivity of crop yield to climate variability leading to both higher mean crop yield (10.3±6.7%) and higher yield stability (decreasing variability by 15.6±14.4%). High-quality soils improve the outcome for yields under climate change by 1.7% (0.5-4.0%), compared to low-quality soils. Climate-driven yield change could result in reductions of national cereal production of 11.4Mt annually under PCR8.5 by 2080-2099. While this production reduction was exacerbated by 14% due to soil degradation; it can be reduced by 21% through soil improvement. This study emphasises the vital role of soil quality in agriculture under climate change.**

Food production may have to increase by as much as 60-100% by 2050 to meet projected food demand due to growing population[1,2]. Growth rates in crop productivity are expected to be driven mainly by technological and agronomic improvements[2-5], as they were during the Green Revolution. However, agriculture now is facing greater challenges than ever before, because increased global food production must be achieved sustainably and under changing global biophysical stressors[6-11].

Climate variability is known to impact crop production. For example, globally, fluctuations in temperature, precipitation or their interaction were found to explain roughly 32–39% of current crop yield variability[12]. Though uncertainties remains about regional and local impacts of climate change, numerous studies have concluded that continued warming will lead to substantial declines in global mean crop yields by the mid-21st century, especially for tropical and sub-tropical agriculture[13-16]. At the same time, there is active debate on where and how such warming will impact agriculture in the temperate zone, such as in China or the United States[17-19]. China is the world's most populous and largest developing country, and agriculture is a fundamental component of its national economy. Agriculture in China feeds ~20% of the global population with only 7% of the world's arable land, and 5% of water resources[5], demonstrating its global importance.

Soil is one of the basic biophysical factors which together with climate determine the major patterns of global agricultural land[20]. Soil quality improvement is recognized increasingly as a fundamental mechanism to increase yield of crops and food insecurity could be made even more acute through continuing soil degradation[10,11]. However, little is known about how interactions between soil and climate change influence the capacity of croplands to produce adequate food supply at regional to national and global scales.

Exploring the interactive effects of soil and climate on agricultural production at regional and global scales is challenging since both are highly heterogeneous. Assessments of the sensitivity of agricultural output to climate variability and change have, to-date, relied either on process-based crop simulation models[21] or empirical and statistical modelling of crop-climate relationships[22,23]. However, both approaches have often neglected the heterogeneity of soil[24], due to the quality and accessibility of regional and/or global soil data in terms of accuracy and range of measured soil characteristics.

Inadequate consideration of soil quality and interactions with climate change impedes our understanding of the food security challenge in the face of rapidly changing biophysical conditions and the implementation of appropriate risk management strategies[24-26]. This is especially true in developing countries, where (a) agriculture is a larger component of gross domestic product; (b) the majority of the world's food-insecure population resides with low-quality and/or severely degraded soil; and (c) the worst effects of climate variability and change on food systems are anticipated[14,21,27]. Similarly, agricultural production in China is also inherently fragile, since it is also endangered by climate change and soil degradation[5,18], and is among the countries most affected by climate change[28].

In this study, we focused on understanding the interaction of climate and soil quality on yield and its variability, using a unique dataset of soil and associated yield observations for 12115 site-years, complemented by multiple climate variables, covering three major crops across major production regions which account for 90% of total cereal production in China (Fig. 1, Table S1). We used a data-driven approach based on a machine learning algorithm to quantify the potential benefits of enhanced soil quality on crop yield and its variability under Best Management Practices ($Yield_{BMPs}$, see Methods section) for both current and future climates.

Yield variation and biophysical explanation

It is well known that yields under farmers' practices are highly variable, especially for smallholder systems, and management practices can be a major cause of this variablity[29,30]. We find that $Yield_{BMPs}$ are also heterogeneous across and within major cropping systems (Extended Data Fig. 1), though best management practices sustainably increased yields by, on average, 10.6% compared to those under farmers' actual practices[4] over the major cropping systems. The yield variations were measured by both standard deviation (SD) and coefficient of variation (CV, SD/mean*100%), with the former termed as absolute stability and the latter as relative stability[31].The CV of $Yield_{BMPs}$ for wheat, maize and rice were 18-22 %, 17-19 % and 13-16 % across systems, which correspond to 1.2 to 1.5 Mg/ha, 1.4 to 1.8 Mg/ha and 1.1 Mg/ha in absolute terms (SD), respectively. The degree of yield variability in this study was higher than that estimated by Ray et al.[12], in which average inter-annual yield variability in China corresponded to 0.7, 0.9 and 0.7 Mg/ha for wheat, maize and rice, respectively. This may be because $Yield_{BMPs}$ variability in the current study was derived from both geographic and decade-scale temporal variation in climate and/or soil conditions[32], in contrast to the inter-annual and climate-induced yield variability considered in Ray et al.[12].

A Gradient Boosted Regression Tree statistical model (GBRT) was used to relate biophysical factors to yield variations for each cropping system. The mean error (E) values were relatively small, and were not significantly different from zero. The average of normalized root mean square errors (nRMSE) ranged from 10.5 – 15.6 % across crops and regions (Table S2), indicating good performance of the GBRT model in modelling yield[33].We also compared the GBRT approach with traditional stepwise multiple linear regression (SMLR) for fitting data. In general, the descriptive statistics indicate a higher level of prediction accuracy of the GBRT than the SMLR (Table S2). In addition to prediction accuracy, GBRT also provides the relative importance of each variable with their partial plots representing the marginal effect of single variables on yields. For all cropping systems excluding winter wheat (W-YZB) and single rice (SR-YZB) in the Yangtze River Basin and maize in northeast China (M-NEC), climatic and soil variables were always ranked among the top four to seven explanatory factors (Extended Data Fig. 2), providing evidence for joint climate-soil control in $Yield_{BMPs}$. However, the most influential bio-physical factors varied among cropping systems. For W-YZB and SR-YZB, and M-NEC, nitrogen (N) rate remains the most important factor in determining yield, showing potential for further improvement in N management (Extended Data Fig. 2).

Buffer effect of high-quality soil to climate variability

To assess the buffering effects of high-quality soil to climate variables, we further established a sub-set of data composed of local pairs of high- and low-quality soils farmed using the same BMPs and under the same climate conditions (see Methods, Extended Data Fig. 3 and 4). High-quality and low-quality soils were grouped according to the two most important and sensitive soil factors and their partial plots in explaining crop- and region-specific yield, based on the above GBRT models (Extended Data Fig. 2, Fig. S1-S3). Dependent upon cropping systems, soil organic matter (SOM), soil available Phosphorus (soil Olsen-P), and/or soil type and soil texture were identified as the most important factors in explaining yield variations (Table S3). The yield stability was compared between the two soil quality groups by measuring both SD and CV. The mean $Yield_{BMPs}$ from high-quality soils were significantly higher, on average by 0.69 Mg/ha across all cropping systems, than those from low-quality soils (Table 1). The SD of yield produced on low-quality soils was either similar or significantly higher than those in high-quality soils (Table 1). Accordingly, the CV in all cropping systems was consistently lower in high-quality soils despite very small differences being found in rice systems, suggesting higher yield stability under high-quality soils. On average, high-quality soils increased relative yield stability compared to low-quality soil by 8.8-51.0% for wheat, 8.8-22.0% for maize and 2.2–12.9% for rice cropping systems (Table 1). Higher yield stability in high-quality soils in wheat and maize cropping systems shows that wheat and maize productivity is more dependent on soil conditions. The lower impacts of soil quality on yield of paddy rice is also expected as the flooding over most of the growing period leads to smaller effects of soil and climatic variables on crop growth.

We further explored how, and to what extent, the total $Yield_{BMPs}$ variations could be explained by climate variables in both high- and low-quality soils. On average, 17.2% (±4.3%) of $Yield_{BMPs}$ variation was explained by climate variability in high-quality soil over all systems excluding late rice in the south of China (LR-SC) and maize in the southwest of China (M-SWC), but the equivalent value was 26.4% (±10.5%) in low-quality soils (Table 1), suggesting that high-quality soil generally reduces the sensitivity of crop production to climate, lowering the climate-driven share of yield variability. Overall, the climate-explained R^2 in those low-quality soils was 1.7 and 1.5 times higher than in good quality soils for wheat and maize, compared with 1.2 times for rice.

Interactions of climate change and soil quality on yield

We derive the yield response to climate change based on the trained GBRT model under future climate conditions (during both 2040-2059 and 2080–2099) following RCP 2.6 and RCP 8.5, assuming no adaptation. The future climate was projected by using the bias-corrected global gridded climate data at 0.5°× 0.5° horizontal resolution from five Earth System Models[34]. Warming is simulated over China even under RCP 2.6 and accompanied by increased precipitation and solar radiation (Fig. S4 and S5). However, depending on region and crop, the effects of climate change on yield in China were diverse, ranging from a decrease by 6.9 % to an increase by 8.6 % over cropping systems, RCPs and periods (Extended Data Fig. 5 and Fig. 6). Generally, cropping systems such as winter wheat in the North China Plain (W-NCP) and late rice in the south of China (LR-SC), benefit from climate change according to the GBRT model. Winter wheat in Yangtze River Basin (W-YZB) and northwest of China (W-NWC), maize in North China Plain (M-NCP), M-SWC and SR-YZB showed yield reductions even in the most positive scenarios of RCP 2.6 (Extended Data Fig. 5). Maize in Northeast of China (M-NEC) showed mixed impacts on yield trends, in contrast to other combinations of RCPs and periods (Extended Data Fig. 5 a,b,c), RCP 8.5 could lead to a decrease in yield during 2080-2099 (Extended Data Fig. 5d). Overall, the negative effects of climate change on yield were more prominent under drastic climate change scenarios at the end of century. Climate change impacts estimated in the current study qualitatively support earlier findings projected using a range of approaches[16,35-37]. China is located in the mid-latitudes and spans temperate, subtropical and tropical climate zones, with very diverse biophysical conditions of arable cropping (Fig. 1, Text S1). Cereal crops are grown either close to temperature thresholds or at suboptimal temperatures, so that a mix of effects of climate change on crop yield over cropping systems and regions was anticipated [18, 21, 38].

Significant interactive effects of soil quality on yield in response to climate change were found in almost all cropping systems across combinations of periods and RCPs, except for M-SWC and SR-YZB (Fig 2). In regions projected to have a negative yield response to climate change, high-quality soils led to smaller yield loss, whereas in regions with positive yield response to climate change, the climate-induced yield increment was larger (Fig. 2, Extended Data Fig. 6). Interestingly, in some cases, especially for wheat, high-quality soil can shift climate-induced yield decreases in low-quality soils to yield increases in high-quality soils (Fig. 2, Extended Data Fig. 6 a,b,c). The significant differences in relative yield change response to climate change between high- and low-quality soils were found in six and five out of nine major cropping systems in middle and at end of century, respectively, with the mean amount of 1.68 % ranging from 0.51 % to 4.02 % across cropping systems, RCPs and periods (Extended Data Fig. 6).

Soil hydrology, soil temperature and evapotranspiration are driven by both climatic and soil factors. High-quality soils (e.g. with medium-textured and high SOM) may better moderate the impact of rainfall variability on soil moisture and crop growth[26,39-41]. Ideally, nutrient additions should be managed to continuously satisfy plant nutrient demand, which requires a thorough understanding of plant requirements and soil nutrient availability[42]. This can be achieved in simulations by assuming that nutrients match demand by setting optimal amount and daily crop demand[21], thus, soil nutrient-related yield variability estimated by a model can be largely underestimated[24]. However, this has proved difficult to achieve in practice because applications must be made before the demand exists[43], and the impulse type management approach, -applying nutrients (particularly N) at key growing stage even in BMPs, fails to match perfectly and dynamically with crop demand in the whole crop growth cycle. Interactive effects of soil P availability and climate in crop production can also be expected, because soil temperature and moisture substantially affect P diffusion, and consequently modulate P bio-availability to the crop[44]. Thus, the nutrient storage and supply capacity provided by soils also enables them to either buffer or reinforce impacts of climate variability and change on crop growth and yield. This could be the underlying mechanism for what we observed in this study, in view of the facts that soil texture, SOM, and/or soil Olsen-P were important factors in classification of soil quality levels. However, the mechanisms by which soil modulates impacts of climate change and variability on crop productivity are highly complex due to the many processes involved[41]. They differed substantially between regions and cropping systems, but to fully disentangle them is beyond the scope of this study.

Production fluctuation derived by climate-soil interactions

Finally, we assessed to what extent climate-derived yield change could be translated into changes in national production fluctuations, and the relative importance of climate-soil interactions. Here, the interactions of soil-climate were the difference in production responses between either a scenario of soil improvement or soil degradation and business as usual (BAU).

Under RCP 2.6, both climate-driven production fluctuations as the sum of total wheat, maize and rice production were small (Fig. 3 a,c). However, high climate forcing scenarios led to more prominent production fluctuations, with annual climate-driven production loss was, on average, 11.4 Mt under RCP 8.5 during 2080-2099, accounting for 3.3% of national total production (Fig. 3 d). This was mainly due to a climate change-driven production loss in wheat in NWC and in wheat and rice in YZB, and in all maize cropping systems, which exceeded the climate change-induced production gain in other cropping systems. Further, under the scenario of all soils being degraded to a low-quality level, the climate change derived annual production loss averaged 13.0 Mt, comprised of 3.8 Mt from wheat, 6.4 Mt from maize and 2.8 Mt for rice (Fig. 3d), accounting for 4.2% of national total wheat, 5.4% of maize and 2.0% of rice production, respectively[45]. These changes in average annual production are similar to the wheat production of some European countries, and higher than the maize production of most African countries[45]. The size of such loss could represent a substantial threat to sustaining the production growth rates necessary to keep up with demand in China, in view of an annual growth rate in cereal production of 3.7% during 1961-2009 in China and 2% globally over the same period[5]. The climate change-derived production loss and risk of short-term food price shocks could be larger, when considering inter-annual variability (Fig. 3). In contrast, if all soils were improved to a high-quality level by 2080-2099, the climate change derived annual production loss could be reduced to 9.0 Mt, with 2.4 Mt for wheat, 3.9 Mt for maize and 2.7 Mt for rice (Fig. 3d). Overall, the interactions of climate and soil accounted for 14% of the climate-driven production loss under BAU under soil degradation and 21% under soil improvement scenarios, respectively.

The soil-climate interaction may be underestimated in the current study, due to other factors not considered here, such as topsoil depth, soil compaction and erosion, and soil biota which could also be important in China[46]. We did not consider elevated [CO_2] and adaptation potential of improved technology, such as improved crop germplasm and adjustment of agricultural structure and planting systems, in assessing both climate-derived yield change and national future production fluctuations. However, these effects could occur on both high- and low-quality soils. We assume that the omission of these factors does not generally challenge conclusions that high-quality soils are better suited to buffer adverse conditions under climate change. However, it must be acknowledged that restoring and/or improving soil quality is a challenging task, especially under warmer climates and more variable precipitation patterns in future, which necessitates a national and international coordinated approach [10, 26].

Increasing production and delivering stable food supplies in a changing and more variable climate requires integrated solutions. We demonstrate here the value of controlled management practice trials on working farms for revealing crop- and region-specific soil and climatic controls on crop production. Our results show that high-quality soils moderate the effects of climate change and climate variability on yield and improve yield stability (Fig. 4). These findings show that improving soil quality could be an effective strategy for increasing the resilience of regional, national and global food production under a changing climate, as a vital component of “climate-smart agriculture”.

Acknowledgements

We thank Dr Jie Pan in Chinese Academy of Agricultural Sciences for her help in projecting future climate by using the global gridded climate data of 0.5°× 0.5° horizontal resolution of five Earth System Models. We thank Prof. Jianchang Yang, Prof. Mingrong He, and Dr. Peng Hou for their help in categorizing types of crop varieties. We also thank Sustainable Agriculture Innovation Network (SAIN) in organizing workshop on soil quality, climate change and food security and discussing early version of manuscript. This work was financially supported by the National Key Research and Development Program of China (2017YFD0200108) and the National Natural Science Foundation of China (31972520) for M.F, L.Q, H.C, Y.M, H.Y, Y.H, W.L. The input of P.S. contributes to the Newton Fund/UKRI-funded project N-Circle (BB/N013484/1). The input of B.E. was supported by the Newton Fund/UKRI-funded project CINAg project (BB/N013468/1). Supplementary information associated with this article can be found in the online version.

Author Contributions:

M.F., designed the research. M.F., L.Q., J.F., R.L., H.C., S.L., F.Z., Y.M., Y.H. R.J., H.Y. W.L., collected data. M.F., L.Q., X.W., P.S., H.C., Y.W., Y.M., contributed to data analysis. M.F., L.Q., wrote the manuscript with edits from X.W., P.S., Y.L., B.E., S.D., T.B. S.P., C.M., All authors read and approved the final manuscript.

Competing interests: The authors declare no competing interests.

Table 1. Observed Mean yield and yield variability (CV) under best management practices ($Yield_{BMPs}$) in high- and low-quality soils and yield variability explained by climate variability for major cropping systems in China.

Crop types	Production regions	Soil quality levels	N	$Yield_{BMPs}$ (Mg/ha)			$Yield_{BMPs}$ variation explained by climate variability (%)
				Mean	SD	CV (%)	
Winter Wheat	North China Plain	High	327	7.1 a*	1.0 b	14.5 b	12.8
		Low	328	6.5 b	1.1 a	17.1 a	19.4
	Yangtze River Basin	High	152	7.0 a	0.9 a	12.5 b	20.1
		Low	158	6.4 b	0.9 a	13.7 a	31.6
	Northwest China	High	106	7.1 a	1.1 b	15.9 b	23.1
		Low	71	5.6 b	1.8 a	32.4 a	42.6
Maize	Northeast China	High	102	10.0 a	1.4 b	14.6 b	20.3
		Low	92	9.2 b	1.5 a	16.0 a	36.7
	North China Plain	High	180	8.3 a	1.1 b	13.1 b	16.3
		Low	175	7.8 b	1.3 a	16.8 a	20.0
	Southwest China	High	130	8.1 a	1.3 b	16.6 b	15.6
		Low	127	7.4 b	1.4 a	19.1 a	14.9
Single rice	Yangtze River Basin	High	241	8.7 a	1.1 a	13.1 b	16.7
		Low	244	8.4 b	1.1 a	13.4 a	18.2
Early rice	South China	High	188	7.1 a	1.0 b	14.2 b	11.2
		Low	184	6.7 b	1.1 a	16.3 a	16.1
Late rice	South China	High	202	7.5 a	0.9 a	12.3 b	17.7
		Low	253	6.6 b	0.9 a	13.1 a	7.4

High- and low-quality soils were grouped according to the two most important and sensitive soil variables in explaining yield variations (See Method and Table S3). N represents the number of paired on-farm trails with different soil quality but the same management practices and climate conditions. $Yield_{BMPs}$ (Mg/ha) are shown as mean, SD (standard deviation), and CV (%, coefficient of variation calculated by dividing mean yield by standard deviation).Climate impacts were assessed by explained variability (R^2) in climate-yield relationship assessed by Gradient Boosted Regression Tree model for high and low soil quality groups. *Different lowercase showed significant difference in mean $Yield_{BMPs}$, SD and CV between high- and low-quality soils for each cropping systems at p=0.05, respectively.

Figure Legends

Fig. 1. Geographical distribution of on-farm trials. a-c, distributions on-farm trials for winter wheat, maize, and rice, respectively. Symbols of purple dot represent on-farm trials. Numbers in brackets indicate the number of on-farm trials for each region of each crop. Map sections of different colours indicate the major wheat, maize, and rice production agroecological regions in China. Harvested area fractions represent the proportion of harvested area of Gridcell (10 km^2) for each crop (Data source: http://www.earthstat.org/). The shade of colour section indicates the size of the harvested area.

Fig. 2. Projected yield change in high- and low- quality soils in future climate change. Projections were conducted under RCP2.6 and RCP8.5 pathways up to 2040-2059 and 2080-2099, and based on Gradient Boosted Regression Tree model trained on sub-data set composed of on-farm trials with paired trials of high- and low-quality soil in major cropping systems in China. Solid lines and diamonds in this figure indicate median and mean yields, respectively; the boundary of the box indicates the 25th and 75th percentile; whisker caps denote the 90th and 10th percentiles. Paired data refer to 585 and 557 for wheat, 412 and 394 for maize, and 631 high- and 681 low-quality soils for rice, respectively. Asterisks represent significant difference in yield change between high- and low-soil quality at $p = 0.10$. W-NCP, winter wheat in North China Plain; W-YZB, winter wheat in Yangtze River Basin; W-NWC, winter wheat in Northwest China; M-NEC, rainfed maize in Northeast China; M-NCP, maize in North China Plain; M-

SWC, rainfed maize in Southwest China; SR-YZB, single rice in Yangtze River Basin; ER-SC, early rice in South China; LR-SC, later rice in South China.

Fig. 3. Climate-change driven change in cereal production. a-d, Climate-change driven change in cereal production of three soil quality scenarios under RCP2.6 (a) and RCP8.5 (b) pathways by 2040-2059, and RCP 2.6 (c) and RCP8.5 (d) by 2080-2099 for major cropping systems in China. The bars (standard deviation, SD) show the average plus inter-annual variability in total cereal production caused by climate change for the three conditions: soil quality maintained at current quality level as business as usual (BAU), soil quality uniformly improved to a high-quality level (SQ improvement), soil quality uniformly degraded to a low-quality level (SQ degradation) for all farmlands of major cropping systems. Green, dark green and light green, columns represent BAU, SQ improvement, and SQ degradation scenarios, respectively. Asterisks refer to cropping systems with significant difference in yield response to future climate changes between high- and low-quality soil at $p = 0.1$. W-NCP, winter wheat in North China Plain; W-YZB, winter wheat in Yangtze River Basin; W-NWC, winter wheat in Northwest China; M-NEC, rainfed maize in Northeast China; M-NCP, maize in North China Plain; M-SWC, rainfed maize in southwest China; SR-YZB, single rice in Yangtze River Basin; ER-SC, early rice in South China; LR-SC, later rice in South China.

Fig. 4. Schematic representation of the pattern of soil quality (SQ) moderating the yield resilience to climate variability and change. High-quality soil leads to higher attainable/mean yield and a less variable response to climate impacts than a low-quality soil. Further, where climate change positively impacts crop yields, then a good quality soil would enhance that positive effect. In contrast, if climate change negatively affects yield, then high-quality soil would at least partially offset those negative impacts.

References

1. Alexandratos, N. & Bruinsma, J. *World Agriculture Towards 2030/2050. The 2012 Revision* (FAO, 2012).

2. Tilman, D. Balzer, C., Hill, J. & Befort, B. L. Global food demand and the sustainable intensification of agriculture. *Proc. Natl. Acad. Sci.* **108**, 20260-20264 (2011).

3. Mueller, N. D. *et al.* Closing yield gaps through nutrient and water management. *Nature* **490**, 254 (2012).

4. Chen, X. *et al.* Producing more grain with lower environmental costs. *Nature* **514**, 486-489 (2014)

5-. Fan, M. S. *et al.* Improving crop productivity and resource use efficiency to ensure food security and environmental quality in China. *J. Exp. Bot.* **63**, 13-24 (2012).

6. Godfray, H. C. J. *et al.* Food security: the challenge of feeding 9 billion people. *Science* **327**, 812-818 (2010).

7. Foley, J. A. et al. Solutions for a cultivated planet. *Nature* **478**, 337 (2011).

8. Porter, J. R. *et al*. *Food security and food production systems* (Cambridge Univ

Press, Cambridge, 2014).

9. Ray, D.K. & Foley, J.A. Increasing global crop harvest frequency: recent trends and future directions. *Environ. Res. Lett.* **8** 044041 (2013).

10. Lal, R. Restoring soil quality to mitigate soil degradation. *Sustainability* **7**, 5875-5895 (2015).

11.Wall, D. & Six, J. *Science* **347**, 695 (2015).

12. Ray, D. K. *et al*. Climate variation explains a third of global crop yield variability. *Nat. Commun.* **6**, 5989 (2015).

13. Battisti, D. S. & Naylor, R. L. Historical warnings of future food insecurity with unprecedented seasonal heat. *Science* **323**, 240-244 (2009).

14. Nelson, G. C. *et al*. *Climate change: Impact on agriculture and costs of adaptation* (Intl Food Policy Res Inst, 2009).

15. Challinor, A. J., Koehler, A. K., Ramirez-Villegas, J., Whitfield, S. & Das, B. Current warming will reduce yields unless maize breeding and seed systems adapt immediately. *Nat. clim. change* **6**, 954 (2016).

16. Zhao, C. *et al*. Temperature increase reduces global yields of major crops in four independent estimates. *Proc. Natl. Acad. Sci.* **114**, 9326-9331 (2017).

17. Schlenker, W., Hanemann, M. & Fisher, A. Will US agriculture really benefit from global warming? Accounting for irrigation in the hedonic approach. *Am. Econ. Rev.* **95**, 395-406 (2005).

18. Piao, S. L. *et al*. The impacts of climate change on water resources and agriculture in China. *Nature* 467, **43** (2010).

19. Ray D. K. *et al.* Climate change has likely already affected global food production. *PloS one* **14**: e0217148 (2019).

20. Ramankutty, N. *et al*. The global distribution of cultivable lands: current patterns and sensitivity to possible climate change. *Global Ecol. Biogeogr.* **11**, 377-392 (2002).

21. Rosenzweig, C. *et al*. Assessing agricultural risks of climate change in the 21st century in a global gridded crop model intercomparison. *Proc. Natl. Acad. Sci.* **111**, 3268-3273 (2014).

22. Lobell, D. B. & Burke, M. B. On the use of statistical models to predict crop yield responses to climate change. *Agr. Forest. Meteorol.* **150**,1443-1452 (2010).

23. Auffhammer, M. & Schlenker, W. Empirical studies on agricultural impacts and adaptation. *Energ. Econ.* **46**, 555-561 (2014).

24. Folberth, C. *et al.* Uncertainty in soil data can outweigh climate impact signals in global crop yield simulations. *Nat. Commun.* **7**, 11872 (2016).

25. Asseng S. *et al.* Uncertainty in simulating wheat yields under climate change. *Nat. Clim. Change* **3**, 827-832 (2013).

26. Basso, B. *et al.* Soil Organic Carbon and Nitrogen Feedbacks on Crop Yields under Climate Change. *Agr. Environ. Letters* **3**, (2018).

27. Müller, C. et al. Implication of climate mitigation for future agricultural production. *Environ. Res. Lett.* **10,** 125004 (2015).

28. IPCC, Climate Change 2022: *Impacts, Adaptation, and Vulnerability. Contribution of Working Group II to the Sixth Assessment Report of the Intergovernmental Panel on Climate Change* (eds. Pörtner, et al.) (Cambridge University Press. In Press, 2022).

29. Zhang, W. *et al*. Closing yield gaps in China by empowering smallholder farmers. *Nature* **537**, 671–674 (2016).

30. Cui, Z. L. *et al.* Pursuing sustainable productivity with millions of smallholder farmers. *Nature* **555**, 363-368 (2018).

31. Knapp, S. & van der Heijden, M. G. A. A global meta-analysis of yield stability in organic and conservation agriculture. *Nat. Commun.* **9**, 3632 (2018)

32. Müller, C. *et al.* Global Gridded Crop Model evaluation: benchmarking, skills, deficiencies and implications. *Geosci. Model Dev. Discuss*, 1-39 (2016).

33. Jamieson, P.D., Porter, J.R. & Wilson, D.R. A test of the computer simulation model ARC-WHEAT on wheat crops grown in New Zealand. *Field Crops Res.* **27**,337–350 (1991).

34. Warszawski, L. *et al*. The inter-sectoral impact model intercomparison project (ISI–MIP): project framework. *Proc. Natl. Acad. Sci.* **111**, 3228-3232 (2014).

35. Xiong, W. *et al*. National level study: the impacts of climate change on cereal production in China. In: *The Impacts of Climate Change on Chinese Agricultur*e-*Phase II Final Report* (AEA Group, 2008).

36. Liu, B. *et al.* Similar estimates of temperature impacts on global wheat yield by three independent methods. *Nat. Clim. Change* **6**, 1130-1136 (2016).

37. Tao, F. *et al*. Global warming, rice production, and water use in China: Developing a probabilistic assessment. *Agr. Forest Meteorol.* **148**, 94-110 (2008).

38. Xiong, W. *et al*. Different uncertainty distribution between high and low latitudes in modelling warming impacts on wheat. *Nat. Food* (2019) doi:10.1038/s43016-019-0004-2

39. Fernandez-Illescas, C. P. Porporato, A. Laio, F. & Rodriguez-Iturbe, I. The ecohydrological role of soil texture in a water-limited ecosystem. *Water Resour. Res.* 37, 2863-2872 (2001).

40. Wang, E. L. *et al*. Capacity of soils to buffer impact of climate variability and value of seasonal forecasts. *Agr. Forest Meteorol.* **149**, 38-50 (2009).

41. Vereecken, H. *et al*. Modeling soil processes: Review, key challenges, and new perspectives. *Vadose Zone J* **15** (2016).

42. Myers, R. J. K. *et al*. The synchronization of nutrient mineralization and plant nutrient demand. In: *The Biological Management of Tropical Soil Fertility* (eds. Woomer, P.I. & Swift, M.J.) (Wiley, Chichester, New York, 1994).

43. Smith, P. & Gregory, P. J. Climate change and sustainable food production. *P. Nutr. Soc.* **72**, 21-28 (2013).

44. Khasawneh, F. E., Sample, E. C., & Kamprath, E. J. (1980). *The role of phosphorus in agriculture* (American Society of Agronomy, Madison, 1980).

45. FAO. FAOSTAT. Statistics Division of the Food and Agriculture Organization of the United Nations http://www.fao.org/faostat/en/#home (FAO, 2006).

46. Fan, M. S. *et al.* Plant-based assessment of inherent soil productivity and contributions to China's cereal crop yield increase since 1980. *Plos One* **8**, e74617 (2013)

Methods

The agroecological zones and major cereal cropping systems

Wheat (*Triticum aestivum L.*), maize (*Zea mays L.*) and rice (*Oryza sativa L.*) are the principal staple foods in China, cultivated across China from cold to subtropical and from arid to semi-arid and humid regions[47]. Nine major cropping systems, accounting for more than 90% of the total production of rice, maize and wheat, were included in the current study. They are defined according to their agroecological and geographical location: 1) winter wheat in North China Plain (W-NCP), 2) winter wheat in Yangtze River Basin (W-YZB), 3) winter wheat in Northwest China (W-NWC), 4) rainfed maize in Northeast China (M-NEC), 5) maize in North China Plain (M-NCP), 6) rainfed maize in Southwest China (M-SWC), 7) single rice in Yangtze River Basin (SR-YZB), 8) early rice in South China (ER-SC), 9) late rice in South China (LR-SC). An overview of the major cropping systems and the geographical distribution of on-farm trials is shown in Fig. 1 and Text S1. A publicly released base map of China was obtained from the Resource and Environmental Data Cloud Platform (http://www.resdc.cn). All map-related operations were performed using ArcGIS 10.8.1 software (www.esri.com/en-us/arcgis).

On-farm trials and data set

A total of 12115 site-year on-farm trials (n=3883 for wheat, 3694 for maize and 4538 for rice) were obtained from the National Soil Test and Fertilizer

Recommendation projects (2005-2013), with sites spread across all the involved agroecological zones (Fig. 1). On-farm trials were conducted to study optimized fertilizer recommendation, in which the three nutrients of N, P and potassium (K) with four rates, and a total of fourteen treatments were included[48]. These experiments were designed and managed by local agricultural experts and/or trained extension officers, and were implemented in on-farm fields. In the present study, only treatments with optimal NPK rates were used, with an exception for LR-SC, for which yield in control plots were used as one of the indicators in classification of soil quality. These optimal NPK treatments were developed specifically to maximise both yield and nutrient use efficiency for a given location based on integrated nutrient management strategies[49], also using locally available practices based on best science and understanding in cultivar choice, sowing date and density, supplementary irrigation (in irrigated cropping systems), weed, insect and disease control (hereafter referred to as BMPs treatments).

Based on these on-farm trials, paired agronomic, climate and soil data sets were established (Table S1). Agronomic data collected according to a standard protocol[48] in the current study included crop varieties, sowing and harvest time, NPK rate, and grain yield of BMPs treatments in each of the on-farm trials. Using yields under locally defined BMPs allowed us to focus on the relative importance of soil quality and climate variability in determining yield and yield variability, and avoiding the impacts of any sub-optimal management impacting yield and its variability. Wheat varieties were classified into small-, medium- and large-spike variety types; Maize and rice varieties were classified into early-, medium- and late-maturity variety types. Soil data consists of soil type, soil texture and SOM, soil Olsen-P and Available-K concentration and pH, which are established indicators of soil quality[50]. Here, soil quality is defined as the capacity of the soil to provide nutrients and water, and to support crop productivity[50]. Soil type was represented as soil genetic classification in China[51] and soil texture was in accordance with USDA texture class, both of which were used as natural genetic attributes. SOM, soil Olsen-P, soil Available-K concentration and pH were measured using standard methods[52], are dynamic over time and represented as manageable soil indicators. Weather data recorded during the crop growing period for each on-farm trial comprised daily mean temperature (Tave), maximum (Tmax) and minimum temperature (Tmin), precipitation (PRE) and sunshine duration (SSD) from the county or municipality where the trial was conducted, and were obtained from the Chinese Meteorological Administration (Table S1). Sunshine duration was converted into daily solar radiation (RAD) using the Weather Aid module in the Hybrid-Maize model (http://www.hybridmaize.unl.edu/). Growing degree days (GDD) was calculated as an annual sum of daily mean temperatures based on sowing and harvest time of BMPs over a base temperature, 0 °C for wheat and 10 °C for maize and rice according to Ramankutty, et al.[20], representing the "growing season length" of crops and which is sufficient to define the cold boundaries of agricultural land[53]. Generally, the present study was built upon the most comprehensive dataset across a wide range of agroecological zones in China. But, the effect of the other omitted variables could have been important in some specific locations.

Explaining yield variation by GBRT

GBRT analysis was performed to assess the relative importance of explanatory variables on $\text{Yield}_{\text{BMPs}}$ variation. The GBRT algorithm is an efficient machine learning method, which combines regression trees and a boosting technique to optimize the predictive performance of multiple single models[54]. The regression tree is a decision tree model that can be used for regression. The specific formula of the decision regression tree shown in Eq.1. $f_i(x)$ is the prediction function for the input variable. $I(x)$ is an indicator function, $I(x)$=1 if $x \in R_m$, and $I(x)$=0 otherwise. R_m indicates partition units of the input space. A regression tree corresponds to a partition of the input space (i.e. feature space) and an output value on these partitioned units. In contrast to a classification tree, the regression tree uses a heuristic method to divide the input space. In the training process, the model traverses all the input variables, finds the optimal segmentation variable j and the optimal segmentation point s to form a partition. In this study, j indicate the elements of input explanatory variables, including 13 to 15 climatic, soil and management variables (Table S1). Suppose that an input space is divided into M units to form a partition of input space $\{R_1, R_2, \ldots, R_M\}$. Each input variable of the model falls on one unit R_m. There is a fixed output value c_m on each unit represents the optimal output value on unit R_m, which is obtained by calculating the average of the output values corresponding to all input instances on R_m. y_i represents the observed $\text{Yield}_{\text{BMPs}}$ for ith on-farm trial.

$$\min_{j,s}\left[\min_{c_1}\sum_{x_i \in R_1(j,s)}(y_i - c_1)^2 + \min_{c_2}\sum_{x_i \in R_2(j,s)}(y_i - c_2)^2\right] \qquad \text{(Eq.1)}$$

$$R_1(j,s) = \{x \mid x^{(j)} \le s\},\ R_2(j,s) = \{x \mid x^{(j)} > s\}$$

$$c_m = \frac{1}{N_m} \sum_{x_i \in R_m(j,s)} y_i \, , x \in R_m, m = 1{,}2$$

$$f_t(x) = \sum_{m=1}^{M} c_m I(x), (x \in R_m)$$

GBRT model obtained by iterating multiple regression trees using stochastic gradient boosting method. Stochastic gradient boosting is a forward stage-wise process, in which a subset of the data is randomly selected to iteratively fit new tree models to minimize the loss function[55](Eq.2.). $f_0(x)$ is the initial regression tree with only one terminal node, estimating a constant value that minimizes the loss function. *L()* is a loss function fitted by least-squares to calculate the residual value between *c* (predicted yield) and y_i (observed yield). $\tilde{y}_{ti}$ refers to residual estimate by negative gradient of the loss function. $f_t(x)$ refer to the *t*th regression tree function for the prediction of dependent variable y, which equal to the sum of the predicted residual value and the predicted value by (*t*-1)th regression tree. Final model $f_T(x)$ is obtained by integrating the results of total *T* regression trees. Boosting generates a final model by shrinking the contribution of each tree and averaging across the final selected set, which is more robust than a single regression tree model and enables fitting of curvilinear functions[54,56].

(1) $f_0(x) = \arg min_c \sum_{i=1}^{N} L(y_i, c)$ (Eq.2)

(2) For $t = 1$ to T do:

$$\tilde{y}_{ti} = -\left[\frac{\partial L(y_i, f_{t-1}(x_i))}{\partial f_{t-1}(x_i)}\right], i = 1{,}2 \cdots N$$

$$f_t(x) = \arg min \sum_{i=1}^{N} L(y_i, \tilde{y}_{t,i})$$

$$\{\mathrm{R_{t,j}}\}_1^{\mathrm{J}} = leaf \;\; region \;\; of \;\; f_t(x)$$

For j=1 to J do:

$$c_{t,j} = \arg min_c \sum_{j=1}^{J} L(y_i, f_{t-1}(x_i) + c)$$

$$f_t(x) = f_{t-1}(x) + \sum_{j=1}^{J} c_{t,j} I(x), (x \in \mathrm{R_{t,j}})$$

(3) Output: $f_T(x) = f_0(x) + \Sigma_{t=1}^{T} \sum_{j=1}^{J} c_{t,j} I\,(x)\ \ (x \in \mathrm{R_{t,j}})$

To run GBRT analysis, four main parameters are needed to define a GBRT algorithm: learning rate (LR), the contribution of each tree to the final fitted model; interaction depth (ID), tree depth and number of iterations; number of trees (NT), integer specifying the total number of trees to fit; bag fraction (BF), the fraction of the training set observations randomly selected to propose the next tree in the expansion. In general, it is suggested that BF is set at around 0.5[55]. Then we set a series of combinations of parameter values (LR and ID) to test GBRT models, thereafter choosing the optimal parameter combination which provided the minimum predictive deviation. These combinations can generate optimal NT using a 10-fold cross-validation method. The relative importance of variables can be estimated based on the number of times a variable is selected for modelling, weighted by the square improvement to each split, and averaged across all trees[57].

We selected climatic, soil and management variables as explanatory variables, and $\mathrm{Yield_{BMPs}}$ as the explained variable to include in the final model. Therefore, the final regression model for each crop was:

$$y_i = F(f_T\,(X_i),Q_i) + \varepsilon_i \qquad \text{(Eq. 3)}$$

(1) y_i represents $\mathrm{Yield_{BMPs}}$ for cropping systems *i*;

(2) $f_T(X_i)$ *is the GBRT function,* $X_i = [C_i, S_i, M_i\,]$, X_i represents input explanatory

variables including climatic variables C_i (Tmax, Tmin, GDD, PRE and RAD), soil variables S_i (Soil type, Soil texture, SOM, Olsen-P, Avail-K and pH) and management variables M_i (application rates of N, P and K);

(3) $Q_i = [LR_i, ID_i, NT_i, BF_i]$, Q_i represents the GBRT model parameters including learning rate (LR_i), interaction depth (ID_i), number of trees (NT_i) and bag fraction (BF_i);

(4) ε_i represents the error.

For each dataset of cropping systems, 10% of the total on-farm trials were randomly excluded to act as independent test datasets. The remaining 90% of trials were used to build GBRT models. To evaluate the robustness of the modelling, we randomly sampled test datasets and run models for 50 times, and evaluated summary statistics of modelling performances (Table S2). GBRT models are developed using the "caret" and "gbm" packages of R software[58], and R scripts are provided by Kuhn & Johnson[59].

The degree of agreement between simulated and observed values was assessed by mean error (E), root mean square error (RMSE), normalized RMSE (nRMSE), which are indices commonly used in both model calibration and validation processes[60]. E is the bias between predicted value and observed value, an index to determine if the model under-(negative) or over-estimates (positive) the observed data[61]. A paired t test was also used to detect whether the E was significantly different from zero[62]. RMSE takes on the same unit of deviation[61], and nRMSE, as a metric of percentage deviation from the average yield, gives a measure of the relative difference of simulated versus observed data. The simulation is considered excellent, good, fair and poor, with nRMSE

< 10%, 10% < nRMSE < 20%, 20%< nRMSE < 30% and nRMSE > 30%, respectively[33].

E, RMSE and nRMSE were calculated according to Eq 4-6:

$$E = \frac{1}{n}\sum_{k=1}^{n}(P_k - O_k) \qquad \text{(Eq. 4)}$$

$$\text{RMSE} = \sqrt{\frac{1}{n}\sum_{k=1}^{n}(P_k - O_k)^2} \qquad \text{(Eq. 5)}$$

$$\text{nRMSE} = \frac{\text{RMSE}}{\bar{O}} \times 100 \qquad \text{(Eq. 6)}$$

Where, P_k and O_k are the predicted and observed yield values at site k, respectively; $\bar{O}$ is the mean of observed yield; n is the number of samples.

Summary statistics of modelling performances for each of the cropping systems are shown in Table S2. The mean E values were relatively small. None of the E values were significantly different from zero. Model evaluation produced average RMSE value ranges of 818-1035 kg ha^{-1} for wheat, 1155-1494 kg ha^{-1} for maize, and 895-996 kg ha^{-1} for rice, which was comparable with those of the latest simulation studies based on multiple site-years dataset [63-66]. Average nRMSE ranged from 10.5 – 15.6 % across three crops and regions, indicating good performance of GBRT model in modelling yield. However, it should be noted that the empirical models are agnostic on the underlying mechanisms. GBRT approach is not exception for this.

Yield response to climate variability in different quality soils

To assess yield resilience to both current climate variability and future change in different quality soils, we developed a sub-set of data composed of locally paired on-farm trials, for high- and low-quality soils in the same climatic conditions and with the same BMPs.

All 6 soil indicators explained integrated yield variations (Extended Data Fig. 2). Thus, we identified the two most important and sensitive soil variables as indicators in grouping high- and low-quality soils in each cropping system. Both soil variables were ranked in the top two of soil factors in explaining yield variation by GBRT (Extended Data Fig. 2), and had strong partial dependence relationships with crop yield (Fig. S1-S3). Then, we divided the entire on-farm trial database based on the two identified soil indicators into “both high”, “both low”, and “low-high”, and “high-low” sub-databases. Without a clear threshold value between yield and manageable soil indicators， high and low value groups were identified according to their mean; when soil type and soil texture were selected as indicators, we divided them into two groups, with half of them as “high” and the remaining half as the “low” group (Table S3). The “both high” and “both low” groups were identified as “high” and “low” quality soil sub-databases, which also were paired with the same management practices and sharing the same climate observed station (Extended Data Fig. 3 and Fig. 4). The increase trends in mean $Yield_{BMPs}$ along soil quality gradients (Fig.S6) suggested that defining soil quality based on two major soil indicators was valid. Further, we grouped low- and high-quality soils based on integrated soil quality index (SQI) and compared yield between two quality levels (Text S2). Difference in yield and yield variation between low- and high-quality soil using the SQI approach was similar to the trend based on sensitive soil variables approach (Table 1 and Table S6). An overall soil quality index is often desired but is actually not very meaningful[50]. However, sensitive soil variables approach allows us to identify feasible soil management practices in diverse crop systems and regions and to contribute to improved soil quality. A final sub-set of data comprised locally paired n=585 high- and 557 low-quality soils for wheat, 412 high- and 394 low-quality soil for maize, and 631 high- and 681 low-quality soil for rice cropping systems (Extended Data Fig. 3).

To assess the yield response to climate variability, we compared mean $Yield_{BMPs}$, SD, and CV between high- and low-quality soils for each cropping system. The SD is termed the absolute yield stability[31]. The CV is termed relative yield stability and captures both changes in the SD and mean of yield across site-years[31,67]. CV of $Yield_{BMPs}$ is calculated using the following equation:

$$CV_{ij}\ (\%) = \frac{SD(Yield_{im})}{Mean(Yield_{im})} \times 100 \qquad \text{(Eq. 7)}$$

Where, SD ($Yield_{im}$)) and Mean ($Yield_{im}$) are Yield variation and mean yield under BMPs of high- and low-quality soil for each cropping system; i and m represent cropping systems and soil quality groups, respectively.

We performed a bootstrapping exercise (1000 bootstrap samples) combined with T-test to assess the statistical significance of differences at P=0.05 in mean yield, SD and CV between high- and low-quality soils for each cropping system.

Furthermore, we used a variation partitioning method to differentiate the relative contribution of climatic variables in explaining yield variation for two soil quality datasets. For each cropping system, two GBRT models were respectively performed with high- and low-quality soil datasets, using Yield-BMPs as the dependent predictor and climatic variables as independent predictors. The relative contribution of climate variability on yield variability was determined by coefficient of determination (R^2), which were estimated through a 10-fold cross validation procedure conducted using the caret:train function[68].

Projecting yield of different quality soil in climate change

For the future climate scenarios, four Representative Concentration Pathways (RCPs), extending to the year 2100 with radiative forcing values from 2.6 to 8.5 Wm^{-2}, were proposed to represent different greenhouse gas emission scenarios[69,70]. In this study, we considered RCP2.6 and RCP8.5. The former represented a very low forcing level and a stringent pathway, peaking in radiative forcing at circa 3 W m^{-2} around the year 2050 and then declining to 2.6 W m^{-2} by 2100; while the latter is a high-end forcing pathway, a continuously increasing radiative forcing pathway to 8.5 W m^{-2} by 2100. We do not explicitly consider RCP 4.5 and RCP 6 assuming results for these pathways would lie between RCP 2.6 and RCP 8.5.

The future climate conditions under RCP 2.6 and RCP 8.5 were projected by using the global gridded climate data of 0.5°× 0.5° horizontal resolution of five Earth System Models (ESMs; GFDL-ESM2M, HadGEM2-ES, IPSL-CM5A-LR, MIROC-ESM-CHEM, NorESM1-M), which were taken from the ISI-MIP Fast Track input-data catalogue[34]. The original data were retrieved from the CMIP5 archive and interpolated and bias-corrected with respect to historical observations by Hempel et al.[71] to remove systematic biases. The CMIP6 models exhibit an improvement in simulation of climate extremes but the model spreads are still comparable between CMIP5 and CMIP6[72], thus we used climate data of CMIP5.

The projected changes in mean Tmax, Tmin, accumulated PRE, and accumulated SSD during the growing season of the major crop growing-areas in both 2040-2059 and 2080-2099 in comparison with 1986–2005 under two RCPs (2.6 and 8.5) are shown in Fig. S4 and S5. RAD and GDD were calculated as described in a previous section. In summary, warming occurs in all seasons even under RCP2.6. Projected Tmax and Tmin on average increased by 1.6℃ and 1.7℃ over major production regions during 2040-2059, then stabilized at a similar level up to 2100 for RCP 2.6 (Fig. S4 a,b); while both Tmax and Tmin increased on average by 2.7℃ and 2.5℃ during 2040-2059, and by 5.6 and 5.1℃ during 2080-2099 for RCP 8.5, respectively (Fig. S5 a,b). Both RCPs show that increases in temperature will be accompanied by increased PRE and SSD during both 2040-2059 and 2080-2099 (Fig.S4 c,d; Fig.S5 c,d), with an exception under RCP2.6 during the 2040-2059 period (Fig. S4 d), when accumulated SSD could decrease for the wheat growing area in NWC. However, PRE and SSD projection show high spatial variability and greater differences between ESMs than temperature.

Yield change was estimated by comparing the yield differences predicted by GBRT models, between future periods (2040-2059 and 2080-2099) and a baseline period (1985-2005) for each cropping system. In running GBRT models, climatic variables were derived from the above climate change scenarios, while soil and management variables used were based either on the whole dataset or on high- and low-soil quality groups. Management and soil variables were paired spatially with projected climate data at 0.5°× 0.5° horizontal resolution. An unpaired t-test was conducted for statistical comparison of yield changes to assess the significance of differences between high and low soil quality groups. Factors tested were considered to be statistically significant at p = 0.10. We also tested the sensitivity of yield change to soil quality by comparing projected yield changes up to 2080-2099 by adjusting data distributions based on the mean soil quality indicator threshold values by -20, -10, +10 and +20%, finding no prominent difference between them (Fig. S7).

To assess further production response derived from interaction of soil and climate for RCP2.6 and RCP8.5 during 2040-2059 and 2080-2099, we established three soil quality scenarios: (1) where soil quality is maintained at the current level as business as usual (BAU), (2) where soil was improved throughout to the high-quality level, and (3) where soil was degraded throughout to the low-quality level for all farmlands of major cropping systems. The definition of high-quality and low-quality soil (Table S1), and projected yield changes per unit area under future climate scenarios (Fig. 2, Extended Data Fig. 5 and 6) were described and shown in the above sections. The total harvested area of each farming system (10^6 ha) was obtained from the China Agriculture Yearbook[73], which is assumed to be maintained the same as at present in the future; thus, the total production response is the product of yield change and harvested area of each of the cropping systems for each of the soil quality scenarios. The interactions of climate-soil were the difference in production responses between either a scenario of soil improvement or soil degradation and BAU.

Data availability

Data that support these findings are available via GitHub (https://github.com/FMS321/soilquality_climatechange_paper.git).

Code availability

Codes for processing the data are available via GitHub (https://github.com/FMS321/soilquality_climatechange_paper.git).

47. Liu, X. & Chen, F. *Farming system in China* (China Agr. Press, Beijing, 2005).

48. Chen, X. P. Using 3414 experiment to establish the index system of soil testing and fertilizer recommendation. In: *Fertilization Technology Highlights* (eds. Zhang, F. S) (Chinese Agricultural University Press, Beijing, China, 2006).

49. Zhang, F. *et al.* Integrated nutrient management for food security and environmental quality in China. *Adv. Agron.* **116**, 1-40 (2012).

50. Bünemann, E.K. *et al.* Soil quality – A critical review. *Soil Biol. Biochem.* **120**, 105-125 (2018).

51. National Soil Survey Office. *Chinese Soil* (China Agriculture Press, Beijing, 1998).

52. Jiang, R. F. & Cui, J. Y. Soil test. In: *Fertilization Technology Highlights* (eds Zhang, F. S) (China Agricultural University Press, Beijing, 2006).

53. Cramer, W.P. & Solomon, A.M. Climatic classification and future global redistribution of agricultural land. *Clim. Res.* **3**, 97-110 (1993).

54. Elith, J., Leathwick, J. R. & Hastie, T. A working guide to boosted regression trees. *J. Anim. Ecol.* **77**, 802-813 (2008).

55. Friedman, J. H. Stochastic gradient boosting. *Comput. Stat. Data An.* **38**, 367-378 (2002).

56. Buston, P. M. & Elith, J. Determinants of reproductive success in dominant pairs of clownfish: a boosted regression tree analysis. *J. Anim. Ecol.* **80**, 528-538 (2011).

57. Friedman, J. H. & Meulman, J. J. Multiple additive regression trees with application in epidemiology. *Stat. Med.* **22**, 1365-1381 (2003).

58. R Development Core Team. R: A Language and Environment for Statistical Computing. R Foundation for Statistical Computing: Vienna, Austria. ISBN 3-900051-07-0, http://www.R-project.org (2018).

59. Kuhn, M. & Johnson, K. *Applied Predictive Modeling* (Springer, Now York, 2013).

60. Yang, J.M., Yang, J.Y. & Liu, S., Hoogenboom, G. An evaluation of the statistical methods for testing the performance of crop models with observed data. *Agric. Syst*. **127**, 81-89 (2014).

61. Loague, K. & Green, R. E. Statistical and graphical methods for evaluating solute transport models: overview and application. *J. Contamin. Hydro.* **7**, 51–73 (1991).

62. Akinremi, O. O. *et al.* Evaluation of LEACHMN under Dryland conditions. I. Simulation of water and solute transport. *Can. J. Soil Sci.* **85**, 223–232 (2005).

63. Palosuo, T. *et al.* Simulation of winter wheat yield and its variability in different climates of Europe: A comparison of eight crop growth models. *Europ. J. Agronomy* **35**,103–114 (2011).

64. Deng, N. *et al.* Closing yield gaps for rice self-sufficiency in China. *Nat. Commun.* **10**,1725 (2019).

65. Correndo, A. A. *et al.* Assessing the uncertainty of maize yield without nitrogen

fertilization. *Field Crops Res.* **260**, 107985 (2021).

66. Rattalino Edreira, J.I. et al., Spatial frameworks for robust estimation of yield gaps. *Nature Food.* **2**, 773–779 (2021).

67. Tilman, D., Reich, P. B. & Knops, J. M. H. Biodiversity and ecosystem stability in a decade-long grassland experiment. *Nature* **441**, 629 (2006).

68. Kuhn, M. Building predictive models in R using the caret package. *J. Stat. Softw.* **28**, 1-26 (2008).69. IPCC. Climate Change 2014: *Climate Change: Synthesis Report* (eds Working Group I, II and III) (Cambridge University Press, Cambridge, 2014).

70. van Vuuren, D. P. *et al*. The representative concentration pathways: an overview. *Clim. Change* **109**, 5-31 (2011).

71. Hempel, S., Frieler, K., Warszawski, L., Schewe, J. & Piontek, F. A trend-preserving bias correction–the ISI-MIP approach. *Earth Syst. Dynam.* **4**, 219-236 (2013).

72. Chen, H., Sun, J., Lin, W., Xu, H., Comparison of CMIP6 and CMIP5 models in simulating climate extremes. *Sci. Bull.* **65**, 1415–1418 (2020).

73. Editorial Board of China Agriculture Yearbook. *China Agriculture Yearbook* (China Agriculture Press, Beijing, 2005).

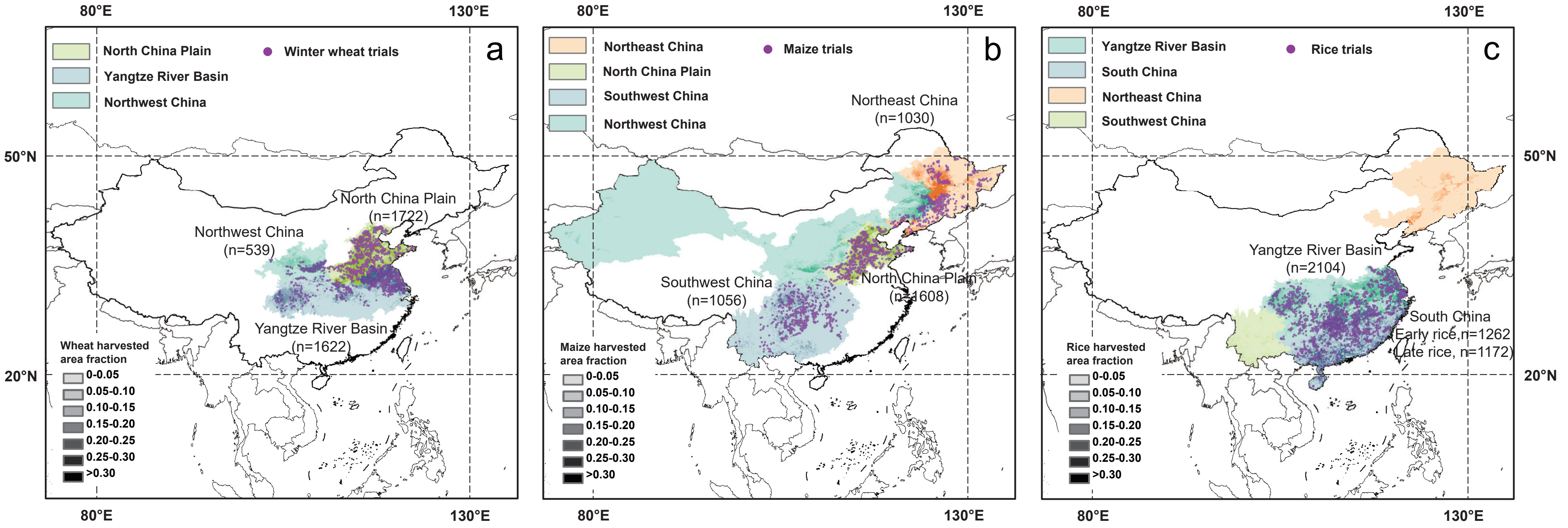

80°E
130°E
50°N
20°N
a
North China Plain
Yangtze River Basin
Northwest China
Winter wheat trials
North China Plain (n=1722)
Northwest China (n=539)
Yangtze River Basin (n=1622)
Wheat harvested area fraction
0-0.05
0.05-0.10
0.10-0.15
0.15-0.20
0.20-0.25
0.25-0.30
>0.30
b
Northeast China
North China Plain
Southwest China
Northwest China
Maize trials
Northeast China (n=1030)
Southwest China (n=1056)
North China Plain (n=1608)
Maize harvested area fraction
c
Yangtze River Basin
South China
Northeast China
Southwest China
Rice trials
Yangtze River Basin (n=2104)
South China Early rice,n=1262 Late rice, n=1172)
Rice harvested area fraction

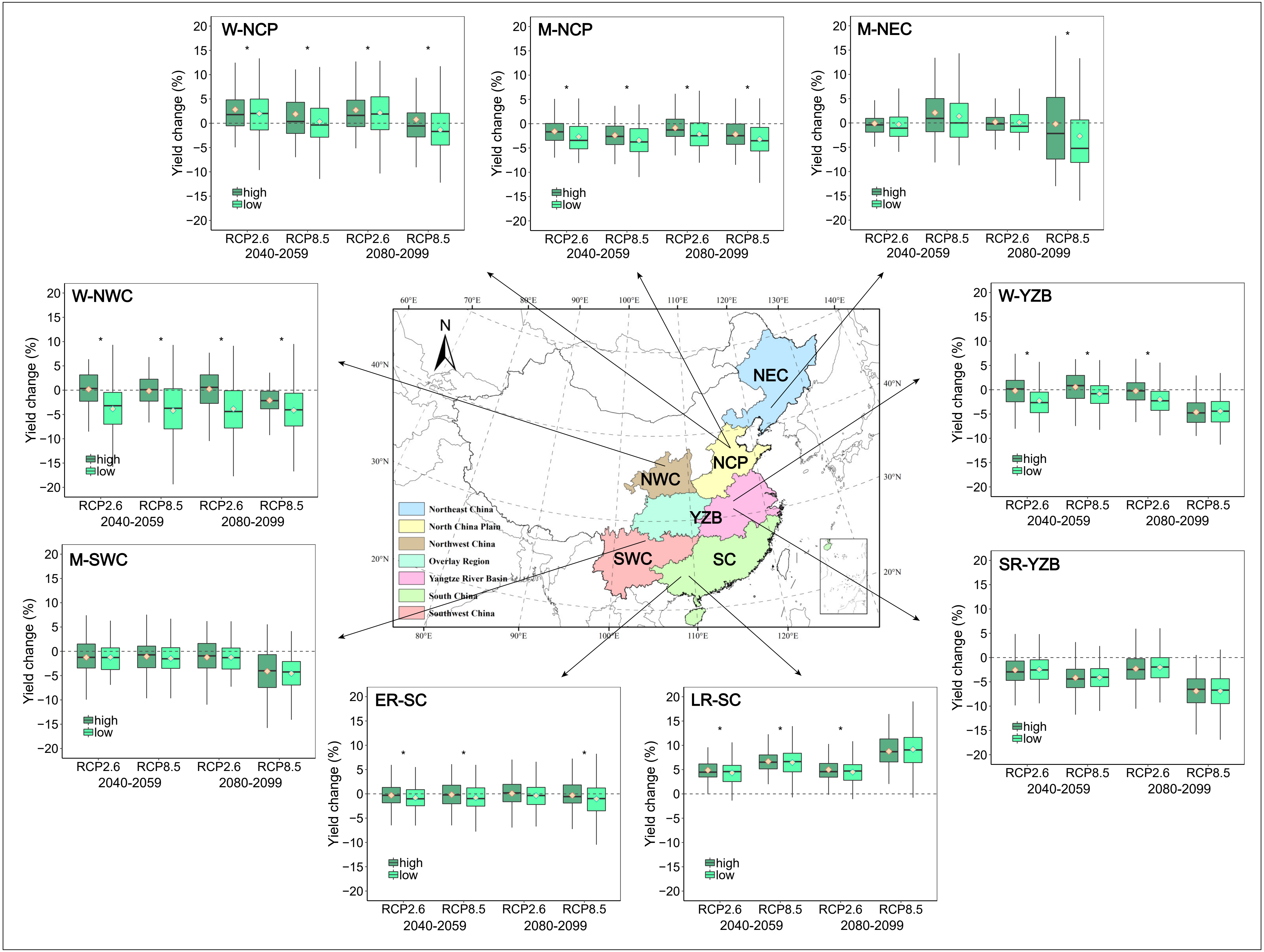
W-NCP
M-NCP
M-NEC
W-NWC
W-YZB
M-SWC
SR-YZB
ER-SC
LR-SC
Yield change (%)
high
low
RCP2.6
RCP8.5
2040-2059
2080-2099
N
NEC
NCP
NWC
YZB
SWC
SC
Northeast China
North China Plain
Northwest China
Overlay Region
Yangtze River Basin
South China
Southwest China

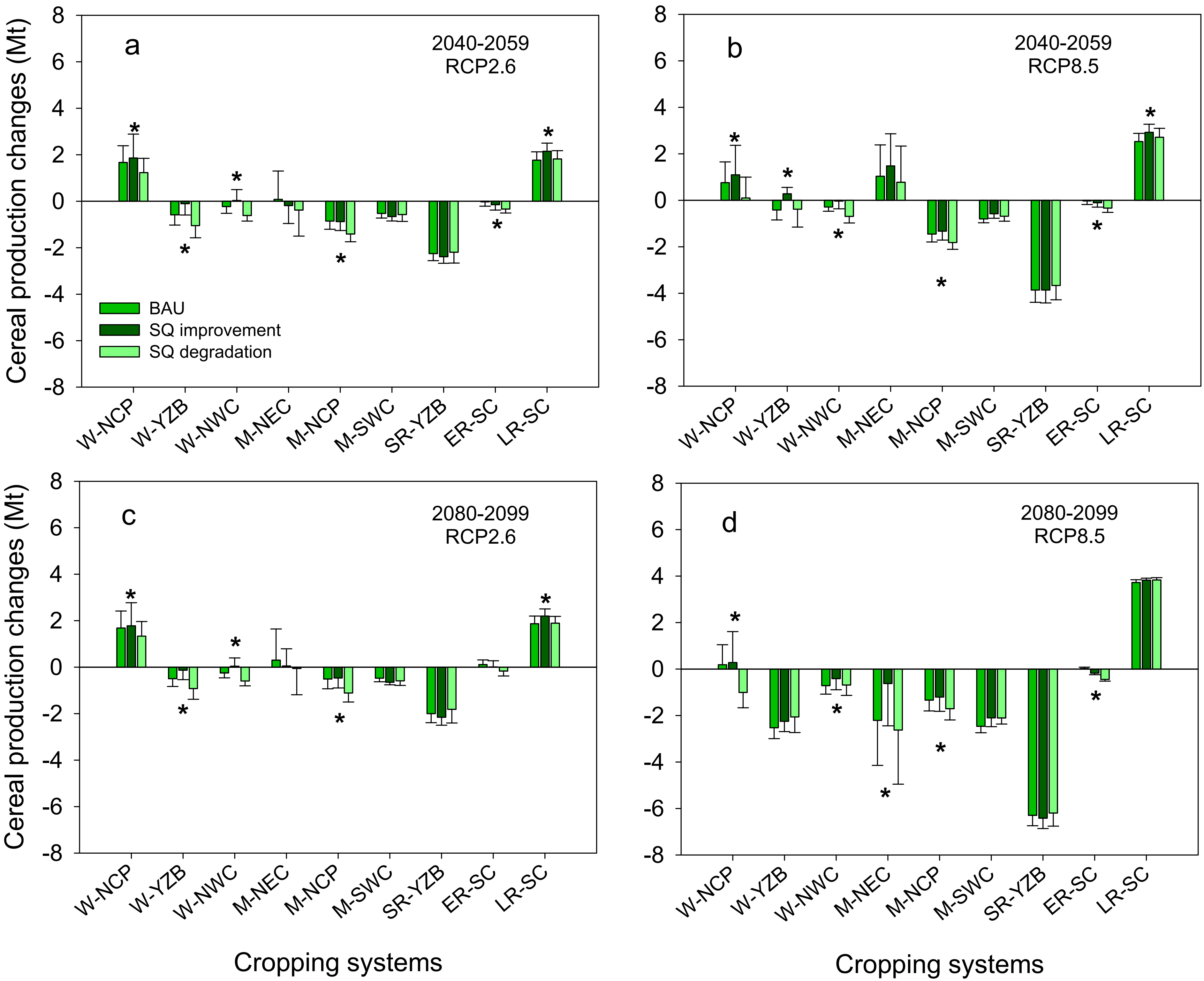

a
2040-2059
RCP2.6
b
2040-2059
RCP8.5
c
2080-2099
RCP2.6
d
2080-2099
RCP8.5
BAU
SQ improvement
SQ degradation
Cereal production changes (Mt)
Cropping systems
W-NCP
W-YZB
W-NWC
M-NEC
M-NCP
M-SWC
SR-YZB
ER-SC
LR-SC

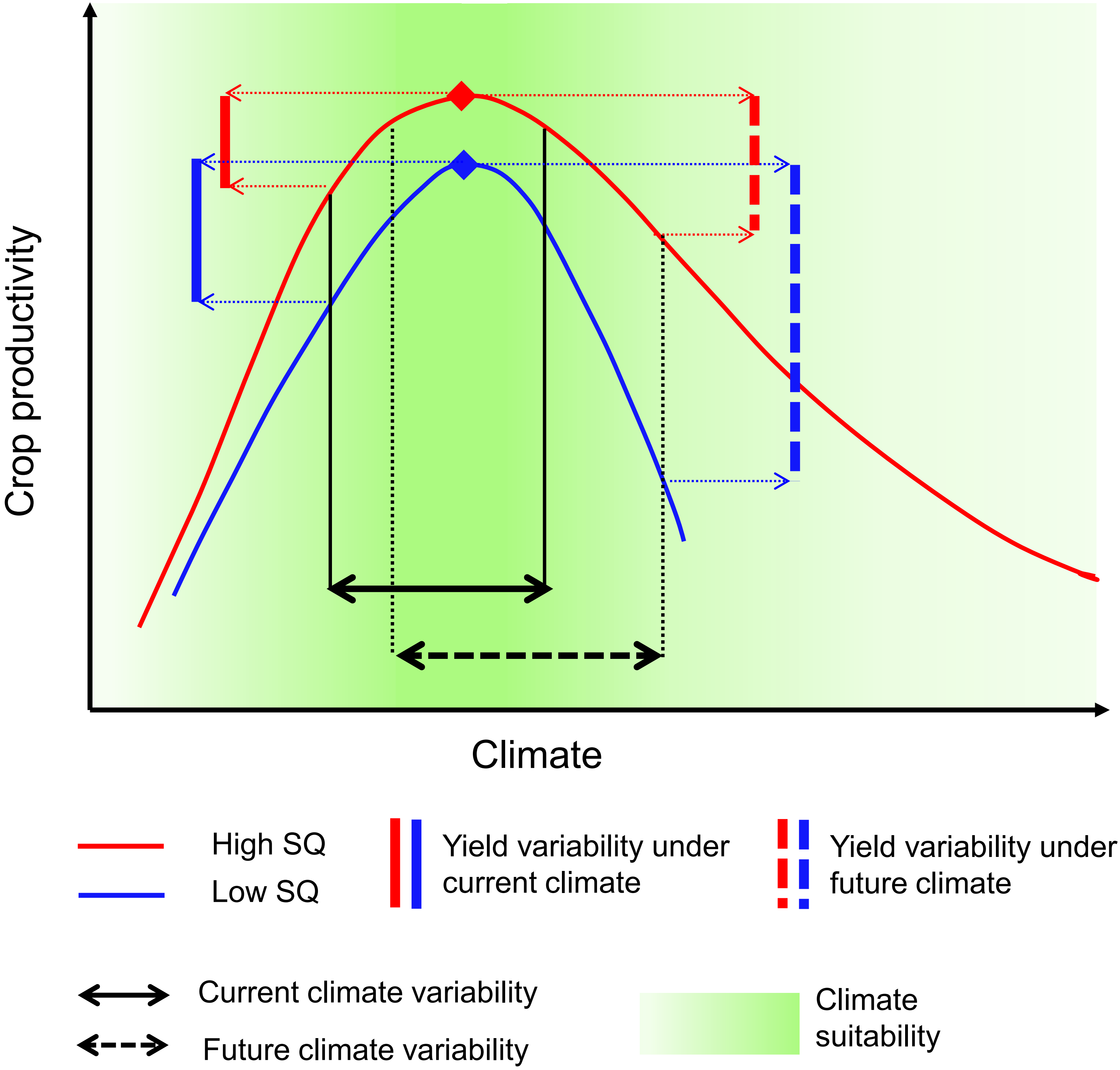

Crop productivity
Climate
High SQ
Low SQ
Yield variability under current climate
Yield variability under future climate
Current climate variability
Future climate variability
Climate suitability

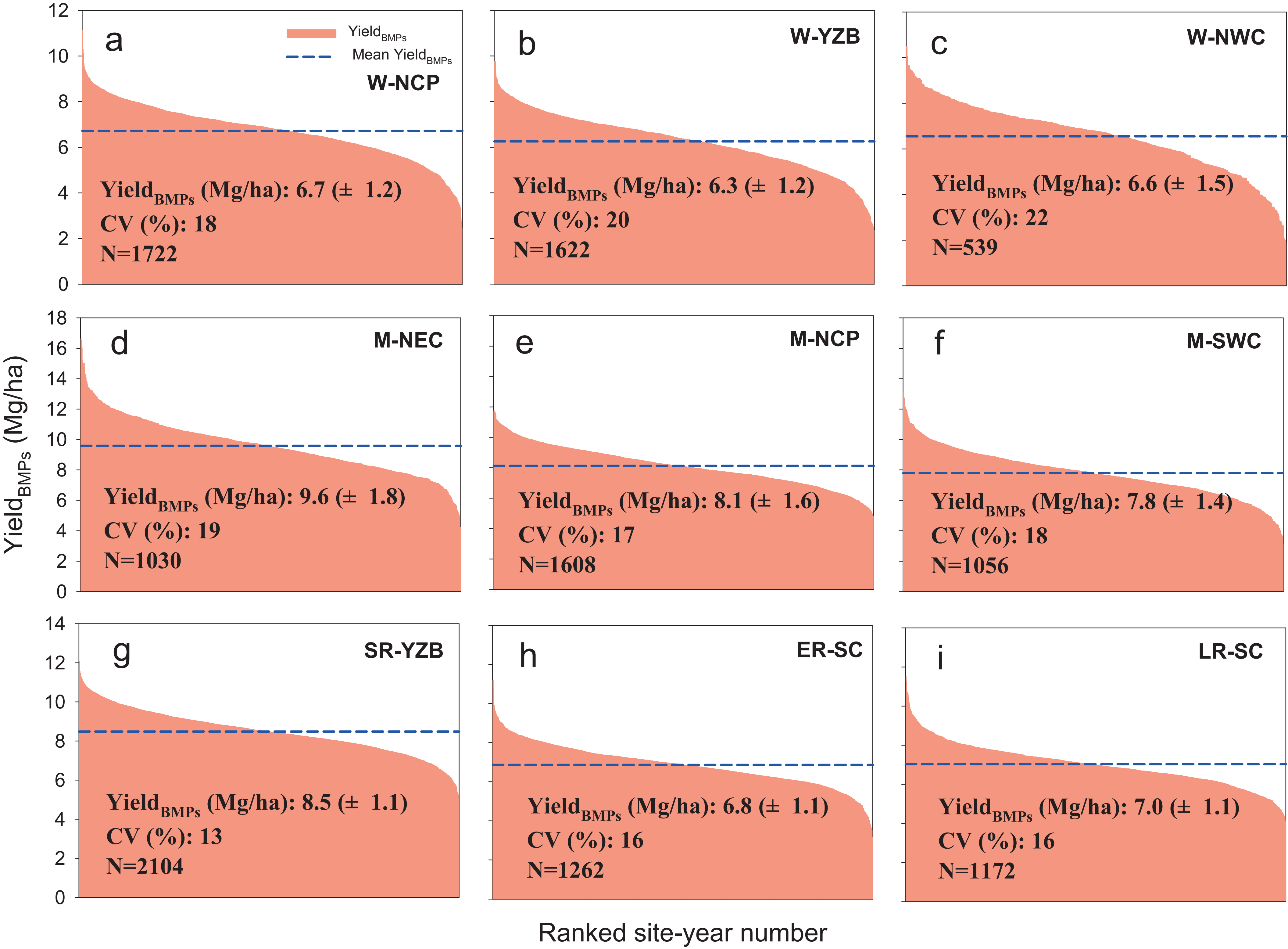

Yield_BMPs
Mean Yield_BMPs
a
W-NCP
Yield_BMPs (Mg/ha): 6.7 (± 1.2)
CV (%): 18
N=1722
b
W-YZB
Yield_BMPs (Mg/ha): 6.3 (± 1.2)
CV (%): 20
N=1622
c
W-NWC
Yield_BMPs (Mg/ha): 6.6 (± 1.5)
CV (%): 22
N=539
d
M-NEC
Yield_BMPs (Mg/ha): 9.6 (± 1.8)
CV (%): 19
N=1030
e
M-NCP
Yield_BMPs (Mg/ha): 8.1 (± 1.6)
CV (%): 17
N=1608
f
M-SWC
Yield_BMPs (Mg/ha): 7.8 (± 1.4)
CV (%): 18
N=1056
g
SR-YZB
Yield_BMPs (Mg/ha): 8.5 (± 1.1)
CV (%): 13
N=2104
h
ER-SC
Yield_BMPs (Mg/ha): 6.8 (± 1.1)
CV (%): 16
N=1262
i
LR-SC
Yield_BMPs (Mg/ha): 7.0 (± 1.1)
CV (%): 16
N=1172
Yield_BMPs (Mg/ha)
Ranked site-year number

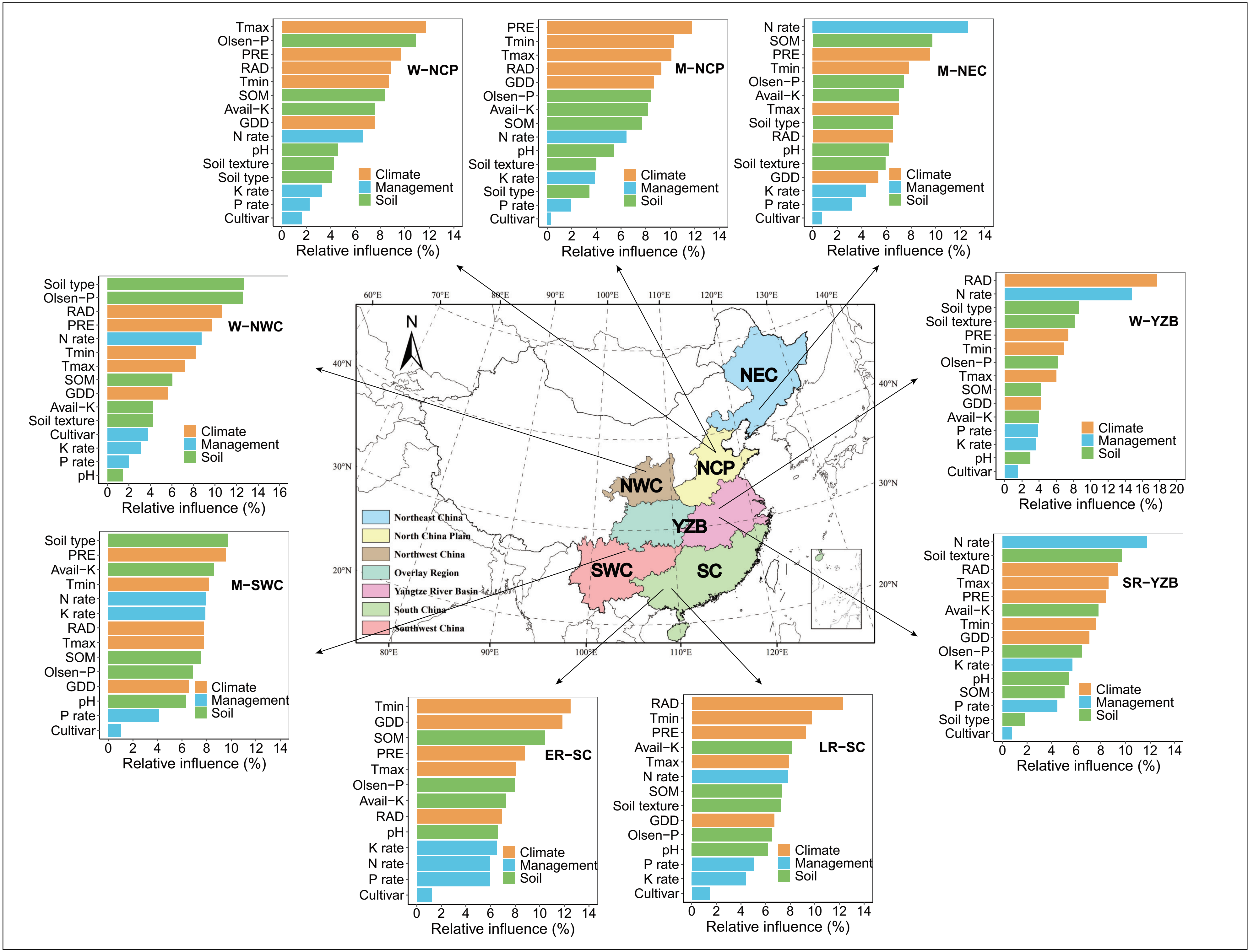

W-NCP
M-NCP
M-NEC
W-NWC
W-YZB
M-SWC
SR-YZB
ER-SC
LR-SC
Relative influence (%)
Climate
Management
Soil
Tmax
Olsen-P
PRE
RAD
Tmin
SOM
Avail-K
GDD
N rate
pH
Soil texture
Soil type
K rate
P rate
Cultivar
NEC
NCP
NWC
YZB
SWC
SC
Northeast China
North China Plain
Northwest China
Overlay Region
Yangtze River Basin
South China
Southwest China
N

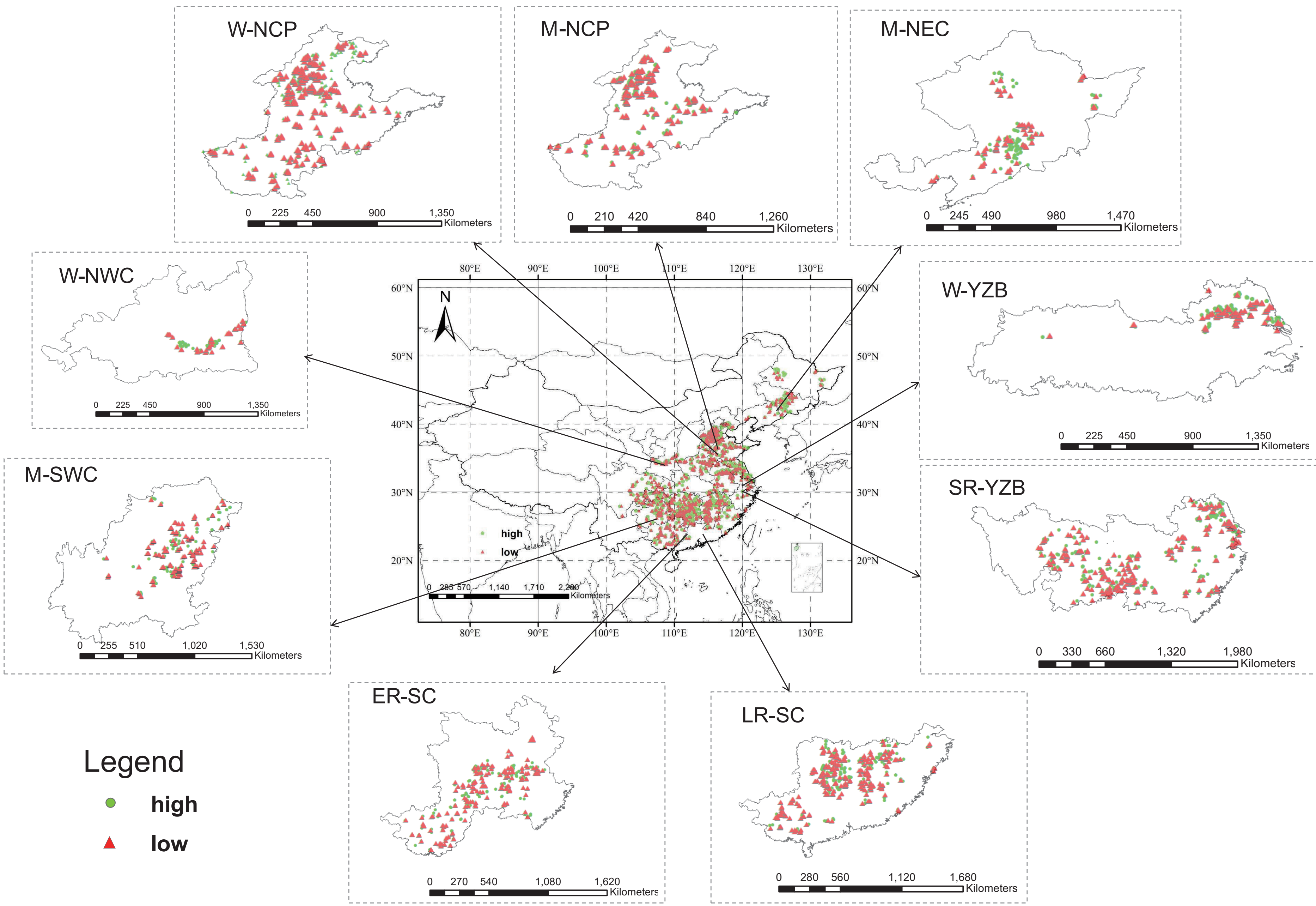
W-NCP
M-NCP
M-NEC
W-NWC
W-YZB
M-SWC
SR-YZB
ER-SC
LR-SC
Kilometers
N
high
low
80°E
90°E
100°E
110°E
120°E
130°E
60°N
50°N
40°N
30°N
20°N
Legend
high
low

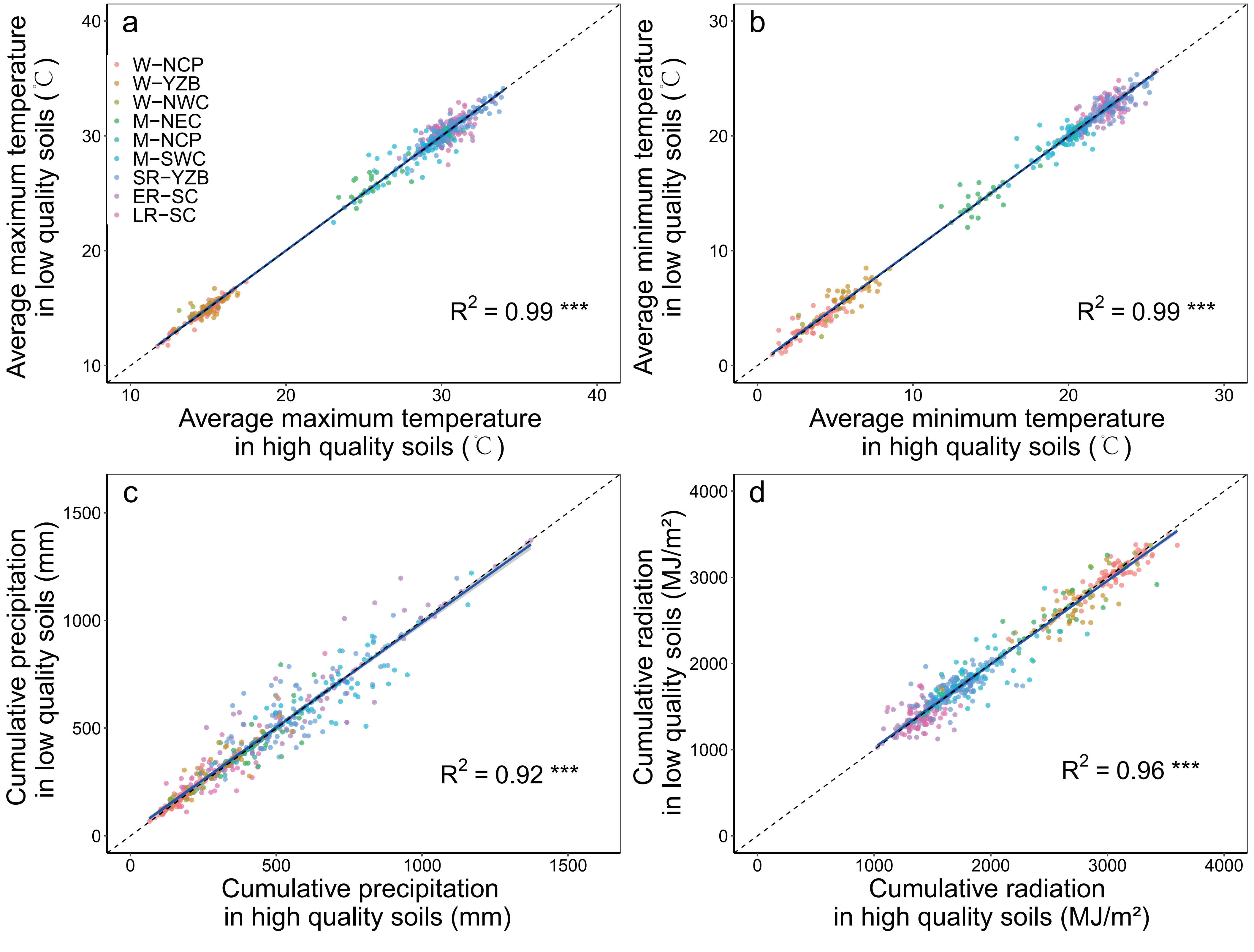
a
W−NCP
W−YZB
W−NWC
M−NEC
M−NCP
M−SWC
SR−YZB
ER−SC
LR−SC
R^2 = 0.99 ***
Average maximum temperature in low quality soils (℃)
Average maximum temperature in high quality soils (℃)
b
R^2 = 0.99 ***
Average minimum temperature in low quality soils (℃)
Average minimum temperature in high quality soils (℃)
c
R^2 = 0.92 ***
Cumulative precipitation in low quality soils (mm)
Cumulative precipitation in high quality soils (mm)
d
R^2 = 0.96 ***
Cumulative radiation in low quality soils (MJ/m²)
Cumulative radiation in high quality soils (MJ/m²)

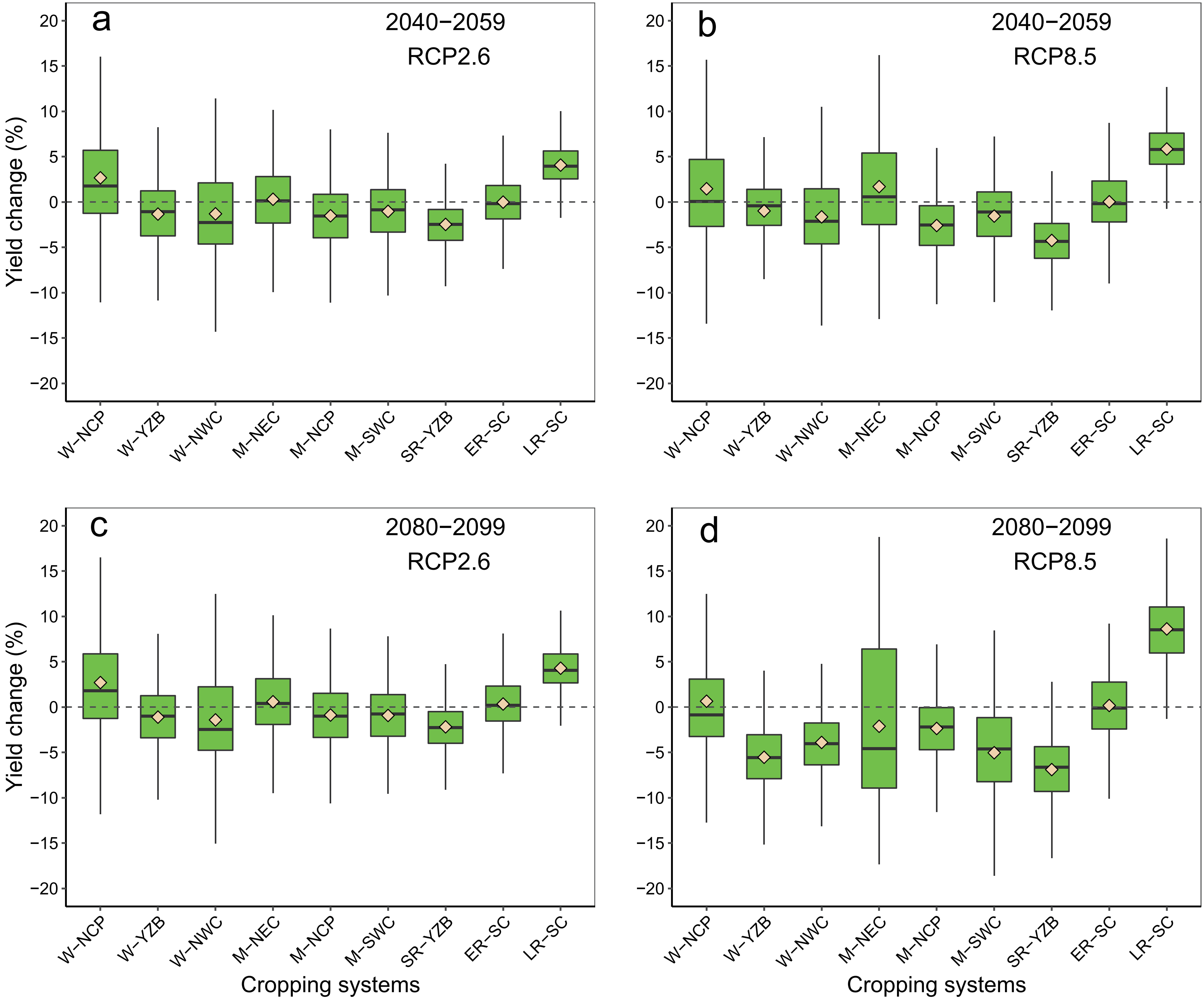

a
2040−2059
RCP2.6
b
2040−2059
RCP8.5
c
2080−2099
RCP2.6
d
2080−2099
RCP8.5
Yield change (%)
20
15
10
5
0
−5
−10
−15
−20
W−NCP
W−YZB
W−NWC
M−NEC
M−NCP
M−SWC
SR−YZB
ER−SC
LR−SC
Cropping systems

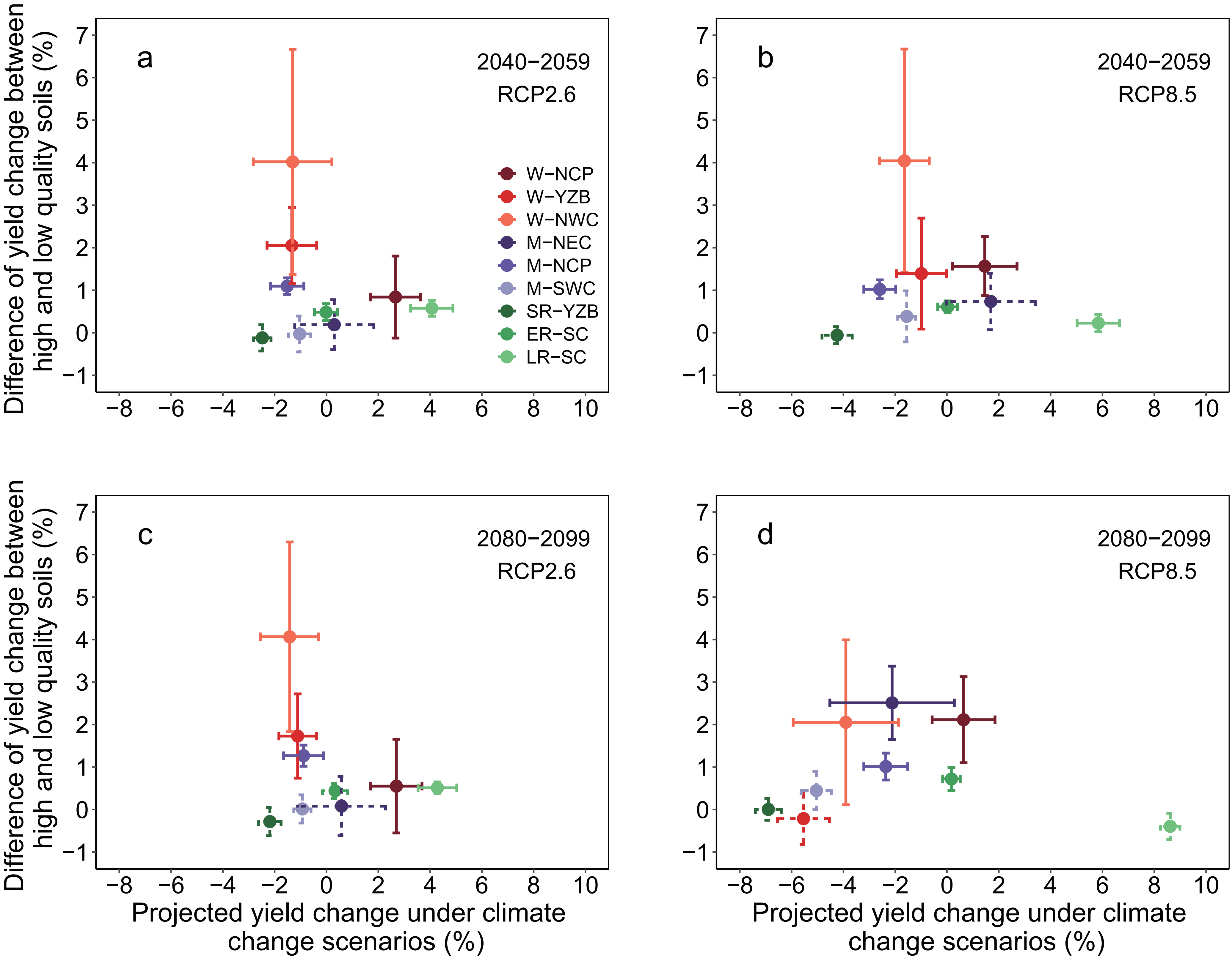
a
2040−2059
RCP2.6
b
2040−2059
RCP8.5
c
2080−2099
RCP2.6
d
2080−2099
RCP8.5
W−NCP
W−YZB
W−NWC
M−NEC
M−NCP
M−SWC
SR−YZB
ER−SC
LR−SC
Difference of yield change between high and low quality soils (%)
Projected yield change under climate change scenarios (%)